

Discrete Dinuclear Cyano-Bridged Complexes

Paul V. Bernhardt,^{*,†} Brendan P. Macpherson,[†] and Manuel Martinez[‡]

Department of Chemistry, University of Queensland, Brisbane 4072, Australia, and Departament de Química Inorgànica, Universitat de Barcelona, Martí i Franques 1-11, E-08028 Barcelona, Spain

Received April 7, 2000

The cyano-bridged complexes $[\text{L}^{14}\text{Co}^{\text{III}}\text{NCFe}^{\text{II}}(\text{CN})_5]^-$, $[\text{L}^{14}\text{Co}^{\text{III}}\text{NCFe}^{\text{III}}(\text{CN})_5]$, $[\text{L}^{15}\text{Co}^{\text{III}}\text{NCFe}^{\text{II}}(\text{CN})_5]^-$, and $[\text{L}^{15}\text{Co}^{\text{III}}\text{NCFe}^{\text{III}}(\text{CN})_5]$ (L^{14} = 6-methyl-1,4,8,11-tetraazacyclotetradecan-6-amine, L^{15} = 10-methyl-1,4,8,12-tetraazacyclopentadecan-10-amine) are prepared and characterized both structurally and spectroscopically. In each complex, the pendant amine is trans to the bridging CN ligand, as determined by spectroscopy and X-ray crystallography: $\text{Na}\{\text{trans}-[\text{L}^{14}\text{Co}^{\text{III}}\text{NCFe}^{\text{II}}(\text{CN})_5]\} \cdot 8\text{H}_2\text{O}$, monoclinic space group $P2_1/c$, $a = 15.58(1)$ Å, $b = 19.797(4)$ Å, $c = 19.830(6)$ Å, $\beta = 91.62(4)^\circ$, $Z = 8$; $\text{trans}-[\text{L}^{14}\text{Co}^{\text{III}}\text{NCFe}^{\text{III}}(\text{CN})_5] \cdot 4\text{H}_2\text{O}$, monoclinic space group $P2_1/m$, $a = 9.9690(9)$ Å, $b = 13.316(1)$ Å, $c = 10.1180(8)$ Å, $\beta = 90.720(6)^\circ$, $Z = 2$; $[\text{L}^{15}\text{Co}^{\text{III}}\text{NCFe}^{\text{III}}(\text{CN})_5] \cdot 4\text{H}_2\text{O}$, triclinic space group $P1$, $a = 9.454(1)$ Å, $b = 9.778(1)$ Å, $c = 9.865(2)$ Å, $\alpha = 60.37(1)^\circ$, $\beta = 62.60(1)^\circ$, $\gamma = 65.82(1)^\circ$, $Z = 1$. A precursor to the 14-membered macrocyclic complexes is prepared for the first time, and its crystal structure is also reported: $\text{trans-I} [\text{CoL}^{14}\text{Cl}](\text{ClO}_4)_2$, orthorhombic space group $Pbca$, $a = 11.833(3)$ Å, $b = 13.363(2)$ Å, $c = 26.015(2)$ Å, $Z = 8$. These compounds form part of a novel series of discrete CN-bridged dinuclear compounds. The mixed-valent $\text{Co}^{\text{III}}-\text{Fe}^{\text{II}}$ compounds exhibit metal-to-metal charge-transfer (MMCT) transitions in the region 510–530 nm.

Introduction

There has been much interest in the field of mixed-valence compounds, especially since the appearance of the classification system devised by Robin and Day¹ and the theoretical treatise on the electronic configurations by Hush.² Prussian Blue, a three-dimensional array of Fe^{III} centers bridged by $[\text{Fe}(\text{CN})_6]^{4-}$ units, has been used as a pigment in inks and dyes since the 18th century because of its intense blue color, which arises from a metal-to-metal charge-transfer (MMCT) transition, whereby an electron is transferred from an Fe^{II} to an Fe^{III} center. The MMCT transition is not possible in the oxidized ($\text{Fe}^{\text{III}}-\text{Fe}^{\text{III}}$) or reduced ($\text{Fe}^{\text{II}}-\text{Fe}^{\text{II}}$) states, resulting in loss of the blue coloration, making these compounds brown and white, respectively. This property of Prussian Blue has also led to an investigation into its possible use in electrochromic devices, which utilize materials that can be electrochemically switched between different colors.³ Possible applications of electrochromic materials include data storage,⁴ solar energy conversion, sensors,⁵ and so-called "smart windows" or displays,³ which are able to modulate light transmittance electronically.

In Prussian Blue and other oligonuclear systems, each electron donor can have as many as six neighboring metal centers that may act as acceptors during the MMCT transition. Each of these

acceptors must be considered in investigations of the electron-transfer processes. The study of discrete dinuclear mixed-valence compounds simplifies such investigations, since an electron-transfer process can involve only one donor–acceptor pair. These compounds are therefore useful tools for probing electron-transfer energetics and electronic coupling interactions between metal centers. A number of dinuclear CN-bridged compounds of the form $[\text{L}_5\text{M}^{\text{III}}\text{NCM}^{\text{II}}(\text{CN})_5]^n$ have been reported with the ligands $\text{L} = \text{CN}^-$ and NH_3 .⁶ Few of the bridged dinuclear mixed-valence compounds reported are robust.⁷ Many are sensitive to oxygen, light, or disproportionation. Although applications of the photolability of some of these compounds have been proposed,⁸ the synthesis of stable compounds is greatly desired.

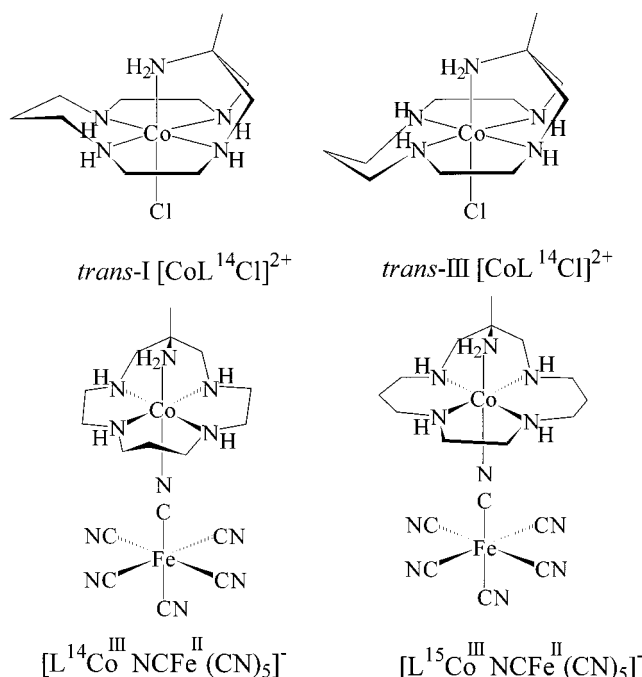
Only two discrete dinuclear CN-bridged hexacyanoferrate compounds have been structurally characterized, both quite recently: $\text{Na}\{\text{trans}-[\text{L}^{15}\text{Co}^{\text{III}}\text{NCFe}^{\text{II}}(\text{CN})_5]\} \cdot 4\text{H}_2\text{O}$ reported by us⁹ (Chart 1) and $[(\text{NH}_3)_5\text{Pt}^{\text{IV}}\text{NCFe}^{\text{II}}(\text{CN})_5] \cdot 6\text{H}_2\text{O}$.¹⁰ In the former case, the cobalt center is coordinated by the pentadentate macrocyclic amine L^{15} . The strong binding of the macrocycle stabilizes the complex and prevents decomposition from the photoexcited ($\text{Co}^{\text{II}}-\text{Fe}^{\text{III}}$) state. We herein report the $\text{Co}^{\text{III}}-\text{Fe}^{\text{III}}$ analogue of this compound and the $\text{Co}^{\text{III}}-\text{Fe}^{\text{II}}$ and $\text{Co}^{\text{III}}-\text{Fe}^{\text{III}}$ analogues of the 14-membered macrocycle, L^{14} .

[†] University of Queensland.[‡] Universitat de Barcelona.

- (1) Robin, M. B.; Day, P. *Adv. Inorg. Chem. Radiochem.* **1967**, *10*, 247.
- (2) Hush, N. S. *Prog. Inorg. Chem.* **1967**, *8*, 391.
- (3) (a) Mortimer, R. J. *Chem. Soc. Rev.* **1997**, *26*, 147. (b) Chang, C.; Ludwig, D.; Bocarsly, A. *Inorg. Chem.* **1998**, *37*, 5467. (c) Granqvist, C. G. *Electrochromism and Electrochromic Devices*. In *The CRC Handbook of Solid State Electrochemistry*; Gellings, P. J., Bouwmeester, H. J. M., Eds.; CRC Press: London, 1997; pp 587–615. (d) Green, M. *Chem. Ind. (London)* **1996**, 641.
- (4) Guihery, N.; Durand, G.; Lepetit, M.-B. *Chem. Phys.* **1994**, *183*, 45.
- (5) Harihar, G.; Rao, G. P. *Sol. Energy Mater. Sol. Cells* **1994**, *33*, 499.

- (6) (a) Haim, A.; Wilmarth, W. K. *J. Am. Chem. Soc.* **1961**, *83*, 509. (b) Vogler, A.; Osman, A. H.; Kunkely, H. *Inorg. Chem.* **1987**, *26*, 2337. (c) Vogler, A.; Kunkely, H. *Ber. Bunsen-Ges. Phys. Chem.* **1975**, *79*, 83. (d) Burewicz, A.; Haim, A. *Inorg. Chem.* **1988**, *27*, 1611. (e) Vogler, A.; Kisslinger, J. *J. Am. Chem. Soc.* **1982**, *104*, 2311.
- (7) Creutz, C. *Prog. Inorg. Chem.* **1983**, *30*, 1.
- (8) Vogler, A.; Osman, A. H.; Kunkely, H. *Coord. Chem. Rev.* **1985**, *64*, 159.
- (9) Bernhardt, P. V.; Martinez, M. *Inorg. Chem.* **1999**, *38*, 424.
- (10) Pfenning, B. W.; Lockard, J. V.; Cohen, J. L.; Watson, D. F.; Ho, D. M.; Bocarsly, A. B. *Inorg. Chem.* **1999**, *38*, 2941.

Chart 1



Experimental Section

Safety Note. Although we have experienced no problems with the compounds reported in this work, perchlorate salts are potentially explosive and should not be heated in the solid state or scraped from sintered-glass frits.

Syntheses. Na₃[Co(CO₃)₃]·3H₂O,¹¹ 6-methyl-1,4,8,11-tetraazacyclotetradecan-6-amine pentahydrochloride (L¹⁴·5HCl)¹² and *trans*-chloro-(10-methyl-1,4,8,12-tetraazacyclotetradecan-10-amine)cobalt(III) perchlorate ([CoL¹⁵Cl](ClO₄)₂)¹³ were synthesized by published methods. All other reagents were obtained commercially and used without further purification.

(a) ***trans*-Chloro(6-methyl-1,4,8,11-tetraazacyclotetradecan-6-amine)cobalt(III) Perchlorate Dihydrate, *trans*-[CoL¹⁴Cl](ClO₄)₂·2H₂O.** Na₃[Co(CO₃)₃]·3H₂O (4.78 g) and L¹⁴·5HCl (5.44 g) were dissolved in ca. 120 mL of water. The color of the solution changed from green to red in ca. 10 min. The red solution was heated at ca. 60 °C for 16 h, diluted to ca. 1 L, and then adsorbed onto a Dowex 50WX2 cation exchange column. The desired product was eluted with 2 M HCl as a single red band. This was reduced to ca. 10 mL on a rotary evaporator, and 2 mL of HClO₄ was added. A red powder precipitated on standing (3.50 g, 55%). Anal. Calcd for C₁₁H₃₁CoCl₃N₅O₁₀: C, 23.65; H, 5.59; N, 12.54. Found: C, 23.16; H, 5.02; N, 12.58. Recrystallization was achieved by dissolving the chloride salt in 20 mL of water and then adding 1 mL of concentrated HClO₄ to afford red X-ray-quality crystals of the diperchlorate on standing. Electronic spectral data (H₂O), λ_{max}, nm (ε, M⁻¹ cm⁻¹): 523 (69), 445 (47), 352 (109). NMR (D₂O): ¹H δ 1.30 (s, 3H, -CH₃), 2.0–3.6 ppm (m, 16 H, -CH₂-); ¹³C, δ 20.7, 30.8, 53.2, 54.6, 55.3, 62.4, 68.0 ppm.

(b) **Na{*trans*-[LⁿCo^{III}NCFe^{II}(CN)₅]} (n = 14, 15) Complexes.** A solution of [CoLⁿCl](ClO₄)₂ (4 mmol; n = 14, 15) in water (200 mL) was adjusted to ca. pH 8 with NaOH, and to this was added K₄[Fe(CN)₆] (1.47 g, 4 mmol). The mixture darkened after ca. 15 min and was then heated at ca. 60 °C for 24 h. The resulting mixture was filtered, and the filtrate, diluted to ca. 2 L, was passed over a Sephadex C-25 cation exchange column to remove any cationic impurities. The desired (anionic) product was not retained by the resin. The eluate was then

adsorbed onto a Sephadex DEAE A-25 anion exchange column (ClO₄⁻ form), and the product was eluted with 0.1 M NaClO₄ solution and reduced in volume on the rotary evaporator to ca. 20 mL.

(i) **Na{*trans*-[L¹⁴Co^{III}NCFe^{II}(CN)₅]}·6H₂O.** Red crystals suitable for X-ray diffraction were formed by vapor diffusion of 2-propanol into a concentrated aqueous solution (0.40 g, 17%). Further crops of the complex could be obtained from the filtrate. Anal. Calcd for C₁₇H₃₉CoFeN₁₁NaO₆: C, 32.3; H, 6.2; N, 24.4. Found: C, 32.8; H, 5.7; N, 24.5. Electronic spectral data (H₂O), λ_{max}, nm (ε, M⁻¹ cm⁻¹): 512 (607), 450 (543), 324 (523). NMR (D₂O): ¹H δ 1.41 (s, 3H, -CH₃), 1.75–3.75 ppm (m, 18H, -CH₂-); ¹³C δ 21.0, 30.8, 52.9, 54.9, 55.1, 62.1, 68.5, 176.9, 178.2, 193.5 ppm. Infrared (KBr disk): ν̄ 2040 (s, equatorial CN), 2074 (m, axial CN), 2119 cm⁻¹ (m, μ-CN).

(ii) **Na{*trans*-[L¹⁵Co^{III}NCFe^{II}(CN)₅]}·12H₂O.** Red crystals suitable for X-ray diffraction were formed by vapor diffusion of acetone into a concentrated aqueous solution (0.40 g, 18%). Anal. Calcd for C₁₈H₅₃CoFeN₁₁NaO₁₂: C, 28.7; H, 7.1; N, 20.5. Found: C, 29.0; H, 6.1; N, 20.5. Electronic spectral data (H₂O), λ_{max}, nm (ε, M⁻¹ cm⁻¹): 528 (420), 462 (370), 326 (410). NMR (D₂O): ¹H δ 1.44 (s, 3H, -CH₃), 2.00–3.30 ppm (m, 20H, -CH₂-); ¹³C, δ 21.9, 26.4, 49.9, 51.1, 54.7, 61.5, 66.6, 177.9, 179.2, 192.1 ppm. Infrared (KBr disk): ν̄ 2042 (s, equatorial CN), 2078 (m, axial CN), 2122 cm⁻¹ (m, μ-CN).

(c) ***trans*-[LⁿCo^{III}NCFe^{II}(CN)₅] (n = 14, 15) Complexes.** To a solution of the corresponding Co^{III}–Fe^{II} compound (0.11 g, 0.1 mmol) in water (10 mL) was added potassium peroxodisulfate (0.06 g, 0.24 mmol). The reaction mixture changed color from red to yellow within ca. 20 min, and yellow crystals suitable for X-ray diffraction formed after ca. 2 h. These were collected by filtration and washed with ethanol. The filtrate became red again upon standing in air for ca. 1 day.

(i) ***trans*-[L¹⁴Co^{III}NCFe^{II}(CN)₅]}·5H₂O.** Anal. Calcd for C₁₇H₃₇CoFeN₁₁O₅: C, 34.6; H, 6.3; N, 26.1. Found: C, 34.28; H, 6.09; N, 26.13. Electronic spectral data (H₂O), λ_{max}, nm (ε, M⁻¹ cm⁻¹): 434 (1150), 407 (1100), 320 (sh, 1100). Infrared (KBr disk): ν̄ 2122 (s, terminal CN), 2131 (w, axial CN), 2164 cm⁻¹ (m, μ-CN).

(ii) ***trans*-[L¹⁵Co^{III}NCFe^{II}(CN)₅]}·6H₂O.** Anal. Calcd for C₁₈H₄₁CoFeN₁₁O₆: C, 34.74; H, 6.64; N, 24.76. Found: C, 34.73; H, 5.65; N, 24.49. Electronic spectral data (H₂O), λ_{max}, nm (ε, M⁻¹ cm⁻¹): 438 (890), 410 (870), 320 (sh, 1100). Infrared (KBr disk): ν̄ 2111 (s, terminal CN), 2125 (w, axial CN), 2172 cm⁻¹ (m, μ-CN).

Physical Methods. Electronic spectra were recorded on a Perkin-Elmer Lambda 40 spectrophotometer, and infrared spectra were obtained on a Perkin-Elmer 1600 Series FTIR spectrometer, with samples in KBr disks. Nuclear magnetic resonance spectra were recorded at 200 (¹H) and 50.3 MHz (¹³C) on a Bruker AC200 spectrometer using D₂O as the solvent and sodium(trimethylsilyl)propionate (TSP) as the reference. A BAS100B/W potentiostat was used for all electrochemistry experiments. DC normal and differential pulse polarographic experiments were performed with an EG&G PARC model 303 dropping-Hg electrode, employing a Pt-wire auxiliary electrode and a Ag/AgCl reference electrode (+220 mV vs NHE). Cyclic voltammetry was performed with either a glassy-carbon working electrode or a static mercury-drop electrode, employing a Pt-wire auxiliary electrode and a Ag/AgCl reference electrode. All aqueous solutions for electrochemistry contained 5 mM analyte and 0.1 M NaClO₄ and were purged with nitrogen gas before measurement. Pulse radiolysis experiments were performed on 10⁻⁴ M solutions of the compounds dissolved in Millipore water. The source of the electron pulse was a linear accelerator at ARPANSA, Yallambie, Australia. The concentration of each solution was such that there was ~10-fold excess of compound to electrons. A 400 W xenon lamp was used as the light source to measure absorbance spectra of the solutions.

Crystallography. Cell constants were determined for all complexes by least-squares fits to the setting parameters of 25 independent reflections measured on an Enraf-Nonius CAD4 four-circle diffractometer employing graphite-monochromated Mo Kα radiation (0.710 73 Å) and operating in the ω–2θ Å scan mode. Data reduction and empirical absorption corrections (ψ-scans) were performed with the XTAL¹⁴

(11) Bauer, H. F.; Drinkard, W. C. *Inorg. Synth.* **1966**, *8*, 202.

(12) Lawrence, G. A.; Manning, T. M.; Maeder, M.; Martinez, M.; O'Leary, M. A.; Patalinghug, W. C.; Skelton, B. W.; White, A. H. *J. Chem. Soc., Dalton Trans.* **1992**, 1635.

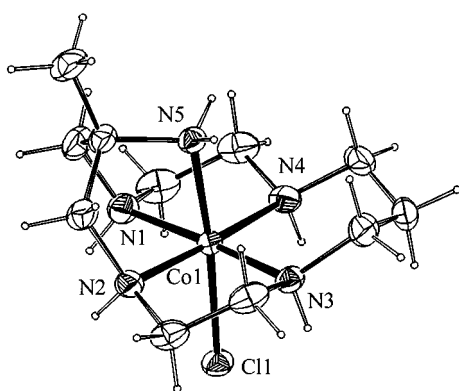
(13) Benzo, F.; Bernhardt, P. V.; Gonzalez, G.; Martinez, M.; Sierra, B. *J. Chem. Soc., Dalton Trans.* **1999**, 3973.

(14) Hall, S. R.; Flack, H. D.; Stewart, J. M., Eds. *The XTAL3.2 User's Manual*; Universities of Western Australia, Geneva, and Maryland: Nedlands, Australia, Geneva, Switzerland; College Park, MD, 1992.

Table 1. Crystal Data

	<i>trans</i> -[CoL ¹⁴ Cl](ClO ₄) ₂	Na[L ¹⁴ Co ^{III} NCFe ^{II} (CN) ₅] ⁺ ·8H ₂ O	[L ¹⁴ Co ^{III} NCFe ^{III} (CN) ₅] ⁻ ·4H ₂ O	[L ¹⁵ Co ^{III} NCFe ^{III} (CN) ₅] ⁻ ·4H ₂ O
formula	C ₁₁ H ₂₇ Cl ₃ CoN ₅ O ₈	C ₁₇ H ₄₃ CoFeN ₁₁ NaO ₈	C ₁₇ H ₃₅ CoFeN ₁₁ O ₄	C ₁₈ H ₃₇ CoFeN ₁₁ O ₄
fw	522.66	667.39	572.34	586.37
space group	<i>Pbca</i> (No. 61)	<i>P2₁/c</i> (No. 14)	<i>P2₁/m</i> (No. 11)	<i>P1</i> (No. 1)
<i>a</i> , Å	11.833(3)	15.58(1)	9.9690(9)	9.545(1)
<i>b</i> , Å	13.363(2)	19.797(4)	13.316(1)	9.778(1)
<i>c</i> , Å	26.015(2)	19.830(6)	10.1180(8)	9.865(8)
α, deg				60.37(1)
β, deg		91.62(4)	90.720(6)	62.60(1)
γ, deg				65.82(1)
<i>V</i> , Å ³	4113.6(1)	6114(5)	1343.0(2)	690.5(2)
<i>Z</i>	8	8	2	1
<i>T</i> , °C	23	23	23	23
λ, Å	0.710 73	0.710 73	0.710 73	0.710 73
μ, cm ⁻¹	12.73	10.88	12.01	11.70
ρ _{calc} , g cm ⁻³	1.688	1.450	1.415	1.410
<i>R</i> (<i>F</i> _o) ^a	0.0445	0.0937	0.0671	0.0686
<i>R</i> _w (<i>F</i> _o ²) ^b	0.1225	0.2488	0.1714	0.1677

$$^a R(F_o) = \sum ||F_o| - |F_c|| / \sum |F_o|. \quad ^b R_w(F_o^2) = [\sum w(F_o^2 - F_c^2)^2 / \sum w F_o^2]^{1/2}.$$

**Figure 1.** View of the *trans*-I [CoL¹⁴Cl]²⁺ cation (30% probability ellipsoids shown).

package. Structures were solved by direct methods with SHELXS-86¹⁵ and refined by full-matrix least-squares analysis with SHELXL-97.¹⁶ The H atoms of noncoordinated water molecules were not modeled. Drawings of the molecules were produced with PLATON97.¹⁷ All non-hydrogen atoms were modeled with anisotropic thermal parameters except for minor contributors to disorder. In the structure of *trans*-[L¹⁴Co^{III}NCFe^{II}(CN)₅]⁺·4H₂O, the complex was found to be disordered about a crystallographic mirror plane, with only atoms C1C, N1C, N6C, and C5 lying in the mirror plane (in addition to O1 and O2 of solvent waters). All other atoms were refined with occupancies restrained to 50%, except O3A and O3B, which were disordered over two independent sites with complementary occupancies. See Table 1 for crystal data and X-ray experimental details.

Results

The precursor complex *trans*-[CoL¹⁴Cl](ClO₄)₂ was prepared in good yield using the [Co(CO₃)₃]³⁻ anion as a reagent. Previously¹² it was found that equilibration of a mixture of L¹⁴ and Co^{II} (over charcoal under a stream of air) leads to the asymmetric *cis* isomer as the dominant product. Only a minor amount of *trans* isomer was found. Interestingly, on the basis of the configurations of the secondary amines, we have identified a *trans* isomer different from that observed previously. The crystal structure of *trans*-[CoL¹⁴Cl](ClO₄)₂ (Figure 1) revealed an *RSSR* (*trans*-I) configuration of the N-donors, resulting in all secondary amine H atoms being on the same side of the

macrocyclic plane. For the *RSSR* (*trans*-III) N-based isomer of *trans*-[CoL¹⁴Cl](ClO₄)₂, the two pairs of amine H atoms share the same six-membered chelate ring on opposite sides of the macrocycle (Chart 1).¹⁸ The Co–N and Co–Cl bond lengths of the *trans*-III¹⁸ and *trans*-I isomers (Table 2) are not significantly different.

The X-ray crystal structure analysis of *trans*-Na[L¹⁴Co^{III}NCFe^{II}(CN)₅]⁺·8H₂O revealed two independent complex anions and sodium counterions in addition to water molecules on general sites. There are no significant differences between the two complex anions, and one of these is shown in Figure 2. The pendant arm of the macrocycle is *trans* to the bridging CN ligand, and the macrocycle retains the *trans*-I N-donor configuration of the precursor chloro pentaamine complex, where the secondary amine H atoms are pointing toward the ferrocyanide moiety. The CN bridge is bent toward the pendant arm of the macrocycle by ca. 10°. The Co–N bond lengths (Table 2) are similar to those found in *trans*-III [CoL¹⁴Cl]²⁺, and the Fe–C bonds are consistent with those found in simple ferrocyanide salts.¹⁹ The equatorial CoN₄ and Fe(CN)₄ coordination planes are eclipsed.

The X-ray crystal structure of the one-electron-oxidized product *trans*-[Co^{III}L¹⁴NCFe^{III}(CN)₅] (Figure 3) revealed the molecule to be disordered about a mirror plane,²⁰ with the bridging CN ligand and the *trans* terminal cyano N atom (N6) lying on the plane. The Fe–C distances are somewhat longer in the Fe^{III} complex, as expected.²¹ Interpretation of the disorder leads to two unique orientations of the equatorial CoN₄ and Fe(CN)₄ planes. However, both conformations are rather similar and each exhibits an essentially eclipsed conformation.

By contrast, the crystal structure of *trans*-[L¹⁵Co^{III}NCFe^{III}(CN)₅]⁻·4H₂O is well ordered (Figure 4). The geometry of the complex bears many similarities to the parent one-electron-reduced complex anion [L¹⁵Co^{III}NCFe^{II}(CN)₅]⁻. The Co^{III}–N bond lengths are the same, indicating that redox reactions at the hexacyanoferrate moiety do not affect the local coordination geometry of the Co^{III} center significantly. However, the two parallel Fe(CN)₄ and CoN₄ coordination planes are almost perfectly staggered, in contrast to the eclipsed conformation of

(15) Sheldrick, G. M. *Acta Crystallogr., Sect. A* **1990**, *46*, 467.

(16) Sheldrick, G. M. *SHELXL-97: Program for Crystal Structure Determination*; University of Göttingen: Göttingen, Germany, 1997.

(17) Spek, A. L. *Acta Crystallogr., Sect. A* **1990**, *46*, C34.

(18) Hambley, T. W.; Lawrance, G. A.; Martinez, M.; Skelton, B. W.; White, A. H. *J. Chem. Soc., Dalton Trans.* **1992**, 1643.

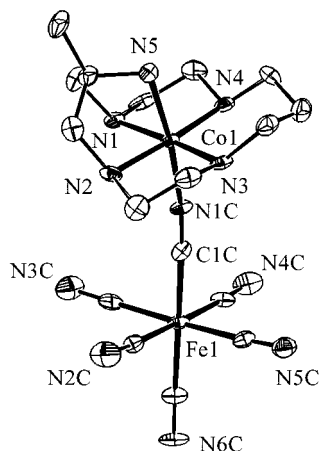
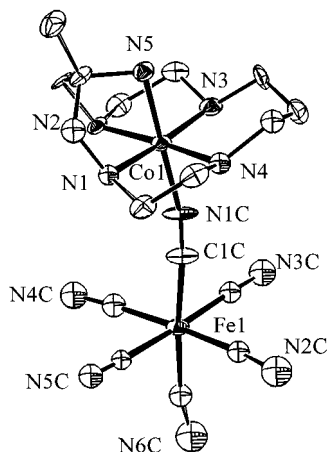
(19) Meyer, H.-J.; Pickart, J. *Acta Crystallogr., Sect. C* **1988**, *44*, 1715.

(20) Both the CoN₆ and Fe(CN)₆ moieties are disordered about the mirror plane. Refinement in the acentric *P2₁* space group gave a significantly poorer *R* value and chemically unreasonable bond lengths.

(21) Marsh, R. E. *Acta Crystallogr., Sect. B* **1995**, *51*, 897.

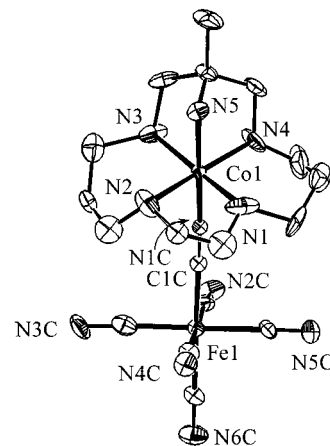
Table 2. Selected Bond Lengths (C) and Angles (E).

	<i>trans</i> -[CoL ¹⁴ Cl](ClO ₄) ₂	Na[L ¹⁴ Co ^{III} NCFe ^{II} (CN) ₅] ⁻ ·8H ₂ O	[L ¹⁴ Co ^{III} NCFe ^{III} (CN) ₅] ⁻ ·4H ₂ O	[L ¹⁵ Co ^{III} NCFe ^{III} (CN) ₅] ⁻ ·4H ₂ O
Co–N1	1.947(3)	1.950(10)	1.912(12)	1.922(17)
Co–N2	1.943(3)	1.943(10)	1.933(11)	1.951(16)
Co–N3	1.951(3)	1.956(10)	1.945(12)	1.980(15)
Co–N4	1.951(3)	1.951(11)	1.942(13)	1.949(16)
Co–N5	1.960(2)	1.946(10)	1.951(10)	1.968(19)
Co–N1C/Cl	2.2467(8)	1.879(10)	1.941(8)	1.897(14)
Fe–C1C		1.879(14)	1.946(10)	1.904(18)
Fe–C2C		1.940(14)	1.88(2)	1.944(19)
Fe–C3C		1.943(17)	1.931(18)	1.93(2)
Fe–C4C		1.884(15)	1.89(2)	1.933(16)
Fe–C5C		1.901(15)	1.98(3)	1.953(19)
Fe–C6C		1.912(14)	1.897(12)	1.95(2)
Co–N1C–C1C		170.8(11)	169.19(6)	172.3(16)
Fe–C1C–N1C		177.1(12)	174.2(5)	171.4(18)

**Figure 2.** View of the *trans*-[L¹⁴Co^{III}NCFe^{II}(CN)₅]⁻ anion (30% probability ellipsoids shown; H atoms omitted).**Figure 3.** View of the *trans*-[L¹⁴Co^{III}NCFe^{III}(CN)₅] molecule (30% probability ellipsoids shown; H atoms omitted).

the Co^{III}–Fe^{II} analogue. The Fe–C bond lengths (Table 2) are slightly longer than those of the Co^{III}–Fe^{II} parent.⁹

The ¹³C NMR spectra of *trans*-Na[L¹⁴Co^{III}NCFe^{II}(CN)₅] and *trans*-Na[L¹⁵Co^{III}NCFe^{II}(CN)₅] show resonances due to the macrocycle in the region 20–70 ppm. All alkyl C atoms have chemical shifts in regions similar to those of the mononuclear cobalt complexes.¹³ The cyano ¹³C NMR resonances are more sensitive to dinuclear complex formation. For the bridged complexes, they are found within the range 170–200 ppm. The ¹³C chemical shift of free cyanide is 166.2 ppm. The chemical shift occurs at 177.2 ppm for [Fe(CN)₆]⁴⁻, which is the only metal cyanide with a chemical shift downfield of free cyanide, due to the strong π-back-bonding of Fe^{II}.²² The four equivalent

**Figure 4.** View of the *trans*-[L¹⁵Co^{III}NCFe^{III}(CN)₅] molecule (30% probability ellipsoids shown; H atoms omitted).

equatorial CN ligands give rise to chemical shifts at 178.2 ppm, close to the value for free ferrocyanide. The axial CN group *trans* to the bridging ligand has a chemical shift close to those of the equatorial CN ligands. The bridging CN ligand resonance is ca. 15 ppm downfield from those of the terminal ligands. This deshielding results from the electron-withdrawing effect of the proximate Co^{III} center.

The solid-state infrared spectra reveal three sets of $\bar{\nu}_{\text{CN}}$ peaks at 2035–2045, 2070–2080, and 2115–2125 cm⁻¹ for the Fe^{II} compounds and at 2110–2130, 2130–2150, and 2160–2170 cm⁻¹ for the Fe^{III} compounds. The lowest frequency peak is the most intense and is assigned to the four equatorial cyanides. A smaller peak, at slightly higher frequency, is assigned to the axial cyanide *trans* to the bridging ligand. The CN–Co bond involves σ-donation from an antibonding orbital, thus strengthening the CN bond and resulting in a higher vibrational frequency. This assignment is consistent with vibrational studies on similar dinuclear CN-bridged compounds.^{23,24} The shift to higher frequency upon oxidation results from weaker π-back-bonding from the Fe^{III} center to the CN π* (antibonding) orbital, leading to higher CN bond order.

Three maxima are observed in the solution electronic spectra of the Co^{III}–Fe^{II} compounds. The bands at ca. 325 and 450 nm are assigned to d–d transitions of Fe^{II} and Co^{III} chromophores

(22) Dunbar, K. R.; Heintz, R. A. *Prog. Inorg. Chem.* **1997**, *45*, 283.(23) (a) Hester, R. E.; Nour, E. M. *J. Chem. Soc., Dalton Trans.* **1981**, 939. (b) Wang, C.; Mohny, B. K.; Williams, R. D.; Petrov, V.; Hupp, J. T.; Walker, G. C. *J. Am. Chem. Soc.* **1998**, *120*, 5848.(24) Nakamoto, K. *Infrared and Raman Spectra of Inorganic and Coordination Compounds*, 4th ed.; John Wiley & Sons: New York, 1986; p 273.

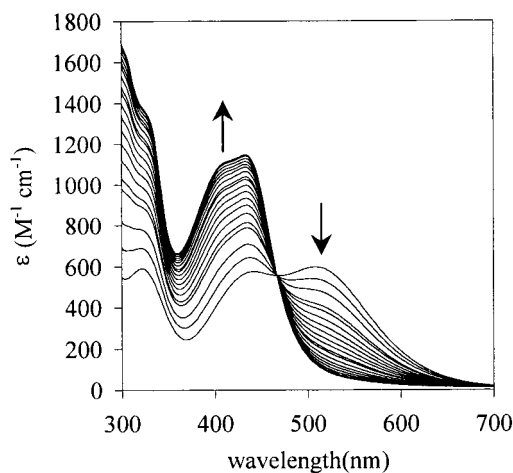


Figure 5. Absorption spectra recorded at 2 min intervals for oxidation of $\text{trans-[L}^{14}\text{Co}^{\text{III}}\text{NCFel(CN)}_5\text{]}^-$ to $\text{trans-[L}^{14}\text{Co}^{\text{III}}\text{NCFel(CN)}_5\text{]}^-$ with $\text{S}_2\text{O}_8^{2-}$ (1 mM aqueous solution of complex; 25 °C).

by comparison with the spectra of mononuclear analogues. The lowest energy d–d transition of $[\text{Fe}(\text{CN})_6]^{4-}$ occurs at 323 nm (ϵ 301 $\text{M}^{-1} \text{cm}^{-1}$).²⁵ Although $[\text{Co}^{\text{III}}\text{N}_5(\text{NC})]^{2+}$ compounds are unstable owing to rapid linkage isomerization to the C-bound form,²⁶ the ligand field strength of the N-bound bridging cyanide has been shown to be comparable to that of amine ligands.²⁷ On this basis, the Co^{III} d–d transitions of $[\text{L}^n\text{Co}^{\text{III}}\text{NCFel(CN)}_5]^-$ ($n = 14, 15$) are expected to be comparable to those of hexamine analogues such as (*trans*-6,13-dimethyl-1,4,8,11-tetraazacyclotetradecane-6,13-diamine)cobalt(III) (λ_{max} 447 and 328 nm).²⁸ Therefore, the maximum at ca. 450 nm in each spectrum is assigned to the lower energy d–d transition of the Co^{III} chromophore and the band at 325 nm to a combination of the d–d bands of Fe^{II} and Co^{III} . The maxima found in the range 510–530 nm for the $[\text{L}^n\text{Co}^{\text{III}}\text{NCFel(CN)}_5]^-$ ($n = 14, 15$) spectra are assigned as MMCT transitions from Fe^{II} to Co^{III} . These bands vanish upon oxidation with $\text{S}_2\text{O}_8^{2-}$. The change in the electronic spectrum with reaction time upon oxidation for $\text{trans-[L}^{14}\text{Co}^{\text{III}}\text{NCFel(CN)}_5]^-$ is shown in Figure 5. The isosbestic point at ca. 470 nm is indicative of a clean redox process involving only two absorbing species.

Cyclic voltammetry of the dinuclear compounds shows two redox waves, which can be assigned to the one-electron oxidations ($\text{Fe}^{\text{III/II}}$) and reductions ($\text{Co}^{\text{III/II}}$) of the parent $\text{Co}^{\text{III}}-\text{Fe}^{\text{II}}$ complex. The $\text{Fe}^{\text{III/II}}$ couples lie within the range 390–435 mV (vs Ag/AgCl) and are totally reversible. The ~ 170 mV shift relative to $[\text{Fe}(\text{CN})_6]^{3-/4-}$ (measured under the same conditions) is a consequence of the adjacent cationic cobalt complex stabilizing the Fe center against oxidation.

Reversibility of the $\text{Co}^{\text{III/II}}$ couples is dependent on the electrode used and the size of the macrocyclic ring. The $\text{trans-[L}^n\text{Co}^{\text{III}}\text{NCFel(CN)}_5]^-$ ($n = 14, 15$) $\text{Co}^{\text{III/II}}$ couples show good reversibility at a Hg working electrode (Figure 6a,c). For comparison, at a scan rate of 100 mV s^{-1} , the anodic/cathodic peak-to-peak separation (ΔE) is greater for $\text{trans-[L}^{15}\text{Co}^{\text{III}}\text{NCFel(CN)}_5]^-$ (163 mV) than for $\text{trans-[L}^{14}\text{Co}^{\text{III}}\text{NCFel(CN)}_5]^-$ (71 mV), indicating slower heterogeneous electron-transfer

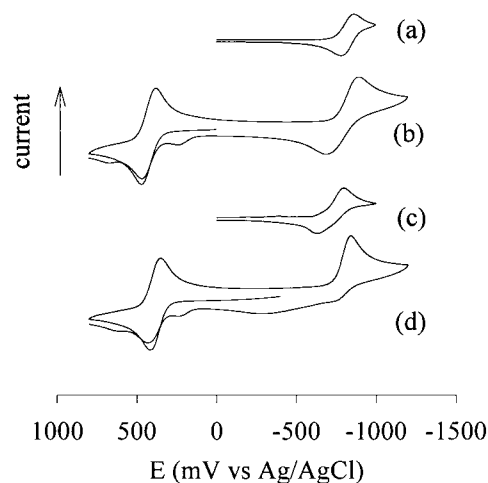


Figure 6. Cyclic voltammograms of (a) $\text{trans-[L}^{14}\text{Co}^{\text{III}}\text{NCFel(CN)}_5\text{]}^-$ (Hg working electrode (WE)), (b) $\text{trans-[L}^{14}\text{Co}^{\text{III}}\text{NCFel(CN)}_5\text{]}^-$ (glassy-carbon WE), (c) $\text{trans-[L}^{15}\text{Co}^{\text{III}}\text{NCFel(CN)}_5\text{]}^-$ (Hg WE), and (d) $\text{trans-[L}^{15}\text{Co}^{\text{III}}\text{NCFel(CN)}_5\text{]}^-$ (glassy-carbon WE). Conditions: scan rate 100 mV s^{-1} ; 5 mM solution of each complex; 25 °C.

kinetics in the complex bearing the larger macrocyclic ring. The anodic/cathodic current ratio (i_a/i_p) is equal to 1 in both cases.

The cyclic voltammograms measured on a glassy-carbon electrode (Figure 6b,d) exhibit quasi-reversible and irreversible $\text{Co}^{\text{III/II}}$ couples for the 14- and 15-membered macrocyclic dinuclear complexes, respectively, and extra waves are seen in the $\text{Fe}^{\text{III/II}}$ region on successive cycles. An extra wave at ca. 220 mV coincides with that of free $[\text{Fe}(\text{CN})_6]^{4-}$, indicating partial dissociation of the compound at this electrode. A wave is also observed at a potential higher than those for the $\text{Fe}^{\text{III/II}}$ couple of the dinuclear complexes, which is assigned to an electrogenerated trinuclear compound bearing two (pentaamine)-cobalt(III) complexes bridged by a ferrocyanide unit.

Single-electron reductions of the $\text{trans-[L}^n\text{Co}^{\text{III}}\text{NCFel(CN)}_5]^-$ ($n = 14, 15$) complexes were achieved with an aquated electron (e_{aq}^-) generated by pulse radiolysis. The electronic spectrum of $\text{trans-[L}^{15}\text{Co}^{\text{II}}\text{NCFel(CN)}_5]^{2-}$ (Supporting Information) shows the disappearance of the MMCT maximum upon reduction, in a manner similar to that seen for the $\text{Co}^{\text{III}}-\text{Fe}^{\text{III}}$ analogue. The absorption bands of the $\text{Fe}^{\text{II}}(\text{CN})_6$ chromophore are unaffected by reduction of the adjacent Co^{III} center.

Discussion

When L^{14} or L^{15} is pentadentately coordinated to an octahedral metal ion, *trans* or *cis* geometric isomers may result depending on the disposition of the pendant amine with respect to the sixth coordination site.^{12,13,18} The *trans* geometry may adopt either a *trans*-I (*RSRS*) or a *trans*-III (*RSSR*) configuration of the secondary amines. This property was first noted for complexes of the unsubstituted relative cyclam (1,4,8,11-tetraazacyclotetradecane).²⁹ Evidently, the *trans*-I isomer of $[\text{CoL}^{14}\text{Cl}]^{2+}$ is the kinetic product and the *cis*- and *trans*-III isomers are the more stable isomers. The synthesis of $\text{trans-[L}^{15}\text{Co}^{\text{III}}\text{NCFel(CN)}_5]^-$ employs the *trans*-II isomer¹³ of $[\text{CoL}^{15}\text{Cl}]^{2+}$ as a precursor, yet the *trans*-III isomer has been identified in the dinuclear product, so N-based isomerization occurs during the dinuclear complex formation.

The mechanism for the formation of $\mu\text{-CN}$ bridged compounds of this type has been well studied.^{30,31} A strongly bound ion pair is formed between the (pentaamine)cobalt(III) cation

(25) Alexander, J. J.; Gray, H. B. *J. Am. Chem. Soc.* **1968**, *90*, 4260.

(26) Halpern, J.; Nakamura, S. *J. Am. Chem. Soc.* **1965**, *87*, 3002.

(27) (a) Shriver, D. F.; Shriver, S. A.; Anderson, S. E. *Inorg. Chem.* **1965**, *4*, 725. (b) De Castello, R. A.; Piriz Mac-Coll, C.; Egen, N. B.; Haim, A. *Inorg. Chem.* **1969**, *8*, 699. (c) De Castello, R. A.; Piriz Mac-Coll, C.; Haim, A. *Inorg. Chem.* **1971**, *10*, 203.

(28) Bernhardt, P. V.; Lawrance, G. A.; Hambley, T. W. *J. Chem. Soc., Dalton Trans.* **1989**, 1059.

(29) Bosnich, B.; Poon, C. K.; Tobe, M. L. *Inorg. Chem.* **1965**, *4*, 1102.

and the ferrocyanide anion ($K > 1000 \text{ M}^{-1}$), which undergoes a rate-determining outer-sphere cross-reaction (Fe^{II} to Co^{III}). The labile Co^{II} pentaamine undergoes ligand substitution by $[\text{Fe}(\text{CN})_6]^{3-}$ at its reactive sixth coordination site (formerly occupied by the Cl^- ligand). In reactions of acyclic pentaamine analogues, this outer-sphere complex typically dissociates, with subsequent precipitation of $\text{Co}^{\text{III}}_3[\text{Fe}^{\text{III}}(\text{CN})_6]_2$. However, in this case, the macrocycles L^{14} and L^{15} stabilize the intermediate $\text{Co}^{\text{II}}\text{--Fe}^{\text{III}}$ dinuclear CN-bridged complex, which undergoes spontaneous back electron transfer to generate the $\text{Co}^{\text{III}}\text{--Fe}^{\text{II}}$ product.

The approximately parallel CoN_4 and $\text{Fe}(\text{CN})_4$ coordination planes of *trans*- $[\text{L}^n\text{CoNCFe}(\text{CN})_5]^{0/-}$ ($n = 14, 15$) can adopt either an eclipsed or a staggered conformation. A number of factors are likely to contribute to the conformation of the coordination spheres adopted by the compounds. In a simple way, steric repulsion between the M–L bonds on the two different coordination planes would favor a staggered conformation, but the separation between the two coordination planes ($> 5 \text{ \AA}$) is too great for any significant intramolecular repulsion to be responsible for a structural change. A possible electronic origin of this geometry change is π -back-bonding from the filled t_{2g} orbitals of each d^6 metal center to the orthogonal π^* molecular orbitals of the bridging CN ligand, which would hold the coordination planes in an eclipsed conformation. Although $\text{Fe}^{\text{II}}\text{--CN}$ back-bonding is significant (evident from crystallographic and IR data), $\text{Co}^{\text{III}}\text{--NC}$ back-bonding should be rather weak by comparison. In the structures of *trans*- $[\text{L}^n\text{Co}^{\text{III}}\text{NCFe}^{\text{III}}(\text{CN})_5]$ ($n = 14, 15$), the 15-membered-ring complex is in a staggered conformation, but the 14-membered analogue is eclipsed. Superimposed on any electronic effects will be crystal packing forces, and it appears that these are an important factor governing the disparate conformations of the two $\text{Co}^{\text{III}}\text{--Fe}^{\text{III}}$ complexes in the absence of significant electronic effects. Quantum mechanical calculations are currently underway that we hope will quantify the electronic energies involved in the staggered and eclipsed conformations. More structurally characterized examples of these complexes will also help to clarify this point.

The d–d transitions of the dinuclear complexes in this work are consistent with isolated hexacyanoferrate(III/II) and hexamminecobalt(III) chromophores. The additional lower energy maxima observed in the spectra of the $\text{Co}^{\text{III}}\text{--Fe}^{\text{II}}$ complexes have been identified as MMCT transitions. Therefore, the *trans*- $[\text{L}^n\text{Co}^{\text{III}}\text{NCFe}^{\text{II}}(\text{CN})_5]^-$ ($n = 14, 15$) complexes fall under the class II category of Robin and Day.¹ The energy of an MMCT transition can be related to the redox potentials of the two metal centers by an equation developed by Hush:²

$$E_{\text{op}} = \Delta E + \chi \quad (1)$$

where E_{op} is the energy of the MMCT transition, ΔE is the energy difference between the two redox isomers ($\text{Co}^{\text{III}}\text{--Fe}^{\text{II}}$

and $\text{Co}^{\text{II}}\text{--Fe}^{\text{III}}$), and χ is the reorganizational energy accompanying electron transfer. The values for χ obtained from the experimental MMCT energies and redox potentials are 9673 and 9838 cm^{-1} for the 14- and 15-membered-macrocylic complexes, respectively. The MMCT half-bandwidth ($\Delta\nu_{1/2}$) is also related to the reorganizational energy according to

$$\Delta\nu_{1/2} = 48.06\chi^{1/2} \text{ cm}^{-1} \quad (2)$$

For the respective 14-membered- and 15-membered-macrocylic dinuclear complexes, the calculated (4727 and 4767 cm^{-1}) and experimental (5563 and 4550 cm^{-1}) half-bandwidths are in good agreement, given the experimental uncertainties in $\Delta\nu_{1/2}$ from the overlapping d–d transitions.

Reduction of the Co^{III} center is not completely reversible, owing to the increased lability of the Co^{II} center of the dinuclear compound, but the macrocycle does enhance the stability of the divalent product in comparison with acyclic analogues. Through pulse radiolysis (a transient technique), we have been able to obtain visible spectra of the reactive *trans*- $[\text{L}^n\text{Co}^{\text{II}}\text{NCFe}^{\text{II}}(\text{CN})_5]^{2-}$ ($n = 14, 15$) species. No Co^{II} d–d transitions could be identified, but the visible-region maxima of (hexaamine)-cobalt(II) ions are typically very weak ($\epsilon < 30 \text{ M}^{-1} \text{ cm}^{-1}$)^{32,33} and these maxima were not distinguishable from the noise in the spectra or overlapping Fe^{II} transitions. However, loss of the MMCT band was quite clear, indicating that the Co center had indeed been reduced.

Conclusions

This report expands the field of structurally characterized hexacyanoferrate bridged dinuclear compounds with the structural characterization of three new examples, where only two had existed previously.^{9,10} The $\text{Co}^{\text{III}}\text{--Fe}^{\text{II}}$ forms of these compounds exhibit MMCT transitions in the range 510–530 nm. The $\text{Co}^{\text{III}}\text{--Fe}^{\text{II}}$ compounds can be reversibly oxidized to their $\text{Co}^{\text{III}}\text{--Fe}^{\text{III}}$ forms, resulting in the loss of the MMCT bands in the electronic spectra and causing a marked change in the color of the compounds from red to yellow. Changing the macrocyclic ring size and donor atoms affects the $\text{Co}^{\text{III/II}}$ redox potential and hence the energy of the MMCT transition. Similarly, Ru or Os may be substituted for the Fe center within the hexacyano moiety in an effort to further tune the MMCT energy, and we are currently pursuing these goals. Applications of these compounds in electrochromic devices such as “smart windows” or optical data storage devices are being pursued.

Acknowledgment. Financial support from the Australian Research Council (Grant 00/ARCL073G), the Australian Institute of Nuclear Science and Engineering, and the Dirección General de Investigación Científica y Técnica (Grant PB97-0914) is gratefully acknowledged.

Supporting Information Available: X-ray crystallographic files, in CIF format, for the structure determinations and electronic spectra of *trans*- $[\text{L}^{15}\text{Co}^{\text{III}}\text{NCFe}^{\text{II}}(\text{CN})_5]^-$ and *trans*- $[\text{L}^{15}\text{Co}^{\text{II}}\text{NCFe}^{\text{II}}(\text{CN})_5]^{2-}$. This material is available free of charge via the Internet at <http://pubs.acs.org>.

IC000379Q

- (30) (a) Miralles, A. J.; Armstrong, R. E.; Haim, A. *J. Am. Chem. Soc.* **1977**, *99*, 1416. (b) Krack, I.; van Eldik, R. *Inorg. Chem.* **1990**, *29*, 1700.
 (31) Martinez, M.; Pitarque, M.-A.; van Eldik, R. *Inorg. Chim. Acta* **1997**, *256*, 51.

- (32) Bernhardt, P. V.; Jones, L. A. *Inorg. Chem.* **1999**, *38*, 5086.
 (33) Creaser, I. I.; Harrowfield, J. M.; Herlt, A. J.; Sargeson, A. M.; Spingborg, J.; Geue, R. J.; Snow, M. R. *J. Am. Chem. Soc.*, **1977**, *99*, 3181.